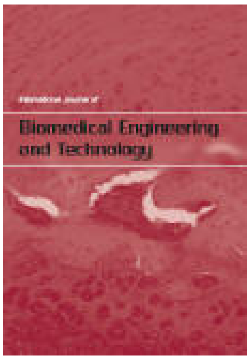

International Journal of Biomedical Engineering and Technology

ISSN online: 1752-6426 - ISSN print: 1752-6418
https://www.inderscience.com/ijbet

Rapid detection of COVID-19 from chest X-ray images using deep convolutional neural networks

Sweta Panigrahi, U.S.N. Raju, Debanjan Pathak, K.V. Kadambari, Harika Ala

DOI: 10.1504/IJBET.2023.10053528

Article History:

Received:	30 May 2020
Last revised:	24 August 2020
Accepted:	21 September 2020
Published online:	25 January 2023

Rapid detection of COVID-19 from chest X-ray images using deep convolutional neural networks

Sweta Panigrahi, U.S.N. Raju*,
Debanjan Pathak and K.V. Kadambari

National Institute of Technology Warangal,
Warangal-506004, Telangana State, India
Email: sweta.panigrahi6@gmail.com
Email: usnraju@nitw.ac.in
Email: debanjan21pathak@gmail.com
Email: kadambari@nitw.ac.in
*Corresponding author

Harika Ala

Institute of Aeronautical Engineering,
Hyderabad, Telangana State, India
Email: bharika85@gmail.com

Abstract: The entire world is suffering from the corona pandemic (COVID-19) since December 2019. Deep convolutional neural networks (deep CNN) can be used to develop a rapid detection system of COVID-19. Among all the existing literature, ResNet50 is showing better performance, but with three main limitations, i.e.: 1) overfitting; 2) computation cost; 3) loss of feature information. To overcome these problems authors have proposed four different modifications on ResNet50, naming it as LightWeightResNet50. An image dataset containing chest X-ray images of coronavirus patients and normal persons is used for evaluation. Five-fold cross-validation is applied with transfer learning. Ten different performance measures (true positive, false negative, false positive, true negative, accuracy, recall, specificity, precision, F1-score and area under curve) are used for evaluation along with fold-wise performance measures comparison. The four proposed methods have an accuracy improvement of 4%, 13%, 14% and 7% respectively when compared with ResNet50.

Keywords: COVID-19 diagnosis; chest X-ray images; deep CNN; transfer learning; cross-validation.

Reference to this paper should be made as follows: Panigrahi, S., Raju, U.S.N., Pathak, D., Kadambari, K.V. and Ala, H. (2023) 'Rapid detection of COVID-19 from chest X-ray images using deep convolutional neural networks', *Int. J. Biomedical Engineering and Technology*, Vol. 41, No. 1, pp.1–15.

Biographical notes: Sweta Panigrahi received her BTech in Computer Science and Engineering from the IIIT Bhubaneswar, Odisha, India in 2014 and MTech in Computer Science and Engineering from the BIT Mesra, Jharkhand, India in 2016. She is currently pursuing her PhD in the Department of Computer Science and Engineering at National Institute of Technology Warangal, India. Her current research area includes computer vision and image processing, object detection, and big image data.

U.S.N. Raju received his BE in CSE from the Bangalore University in 1998, MTech in Software Engineering from the JNT University in 2002 and PhD in CSE from the JNT University Kakinada in 2010. He worked in industry for two years and then in academics for 18+ years. He is presently working in Department of Computer Science and Engineering at the National Institute of Technology Warangal, Telangana State, India since eight years. He is a member of IEEE since seven years and life member of ISTE, CSI, ISCA and IEI. His area of research is big image data processing.

Debanjan Pathak received his BTech in Computer Science and Engineering from the Jalpaiguri Government Engineering College, West Bengal, India in 2014 and MTech in Computer Science and Engineering from the Indian Institute of Technology (Indian School of Mines), Dhanbad, India in 2017. He is currently pursuing his PhD in the Department of Computer Science and Engineering at National Institute of Technology Warangal, India. His current research area includes computer vision and image processing, image retrieval, and big image data processing.

K.V. Kadambari completed her BTech in CS&IT from the PVP Siddhartha Institute of Technology, Vijayawada, Andhra Pradesh, India in 2002. Later on she obtained her MTech from the Andhra University College of Engineering, Visakhapatnam, India in 2004. She obtained her PhD from the School of Computer and Systems Sciences, Jawaharlal Nehru University, Delhi in 2011. Her areas of research include machine learning, neuroimaging and computer vision.

Harika Ala received her BTech in Computer Science and Engineering from the Gates Institute of Technology, Andhra Pradesh, India in 2007 and MTech in Software Engineering from the Rajeev Gandhi Memorial College of Engineering and Technology, Andhra Pradesh, India in 2011. She is currently working as an Assistant Professor at the Institute of Aeronautical Engineering, Hyderabad, India. Her current research area includes medical image processing.

1 Introduction

The entire world is suffering from the corona pandemic (COVID-19) since December 2019. According to WHO (2020a) coverage, COVID-19 is spreading rapidly across the globe. Huang et al. (2020) have found that the coronavirus which originated in Wuhan, China is showing serious pneumonia-like symptoms. This is proving fatal as the death rate is increasing. Nationalgeographic (2020) has found out that this virus not only affects the lungs but the whole body. Worldometers (2020) shows that the COVID-19 victims are in millions. Mahase (2020) has surveyed that COVID-19 is less deadly when compared to SARS and MERS. Even though, COVID-19 has caused more deaths than that of SARS and MERS combined. The economy has also plunged to quite low with a loss in billions. COVID-19 can be transmitted from human to human. The main reason for this rapid spread of COVID-19 is that it can pass from one to another by small droplets which are passed by a coronavirus positive patient when they sneeze, cough or speak. However, the mass of these droplets are heavier than air, so they cannot travel in the air. A person can get infected if these droplets enter the body during breathing. Therefore, people need to maintain a distance of 1 metre from each other. Another source of infection is if a person touches any object which has these droplets on its surface and then if that person touches their mouth, eyes or nose without washing hands. So, another way to prevent the spread of this disease is to clean hands with soap and water or with an alcohol-based sanitiser. WHO (2020b) is researching to know the nature in which COVID-19 is spreading and how to control it. In dealing with COVID-19, a number of scientists and researchers are working in exploring for quick diagnosis, different prevention methods, proper medicine and vaccine for it.

Three different methods can be used to diagnose COVID-19:

a *look for the presence of virus:* RT-PCR test is used for this

b *look for antibodies that arise when a body is attacked by the virus:* antigen test is used for this

c *look for lung damage:* CT images of lungs or chest X-ray images can be used in this test.

Technology Networks (2020) has specified that the RT-PCR tests are accurate but takes too much time, energy and trained personal to run tests. Sciencemag (2020) has reported that the problem with antigens is that in the case of respiratory viruses often there is not enough of the antigen material present in the nasal swab to be detectable. Zu et al. (2020) have determined that radiograph images such as X-rays can be analysed to get early detection of COVID-19. Several key features can help detect COVID-19. Wong et al. (2020) conducted a study that reported that radiograph images of COVID-19 positive patients show ground-glass opacity (GGO). Kong and Agarwal (2020) found that radiograph images of COVID-19 patients also show a right infrahilar airspace opacity. Yoon et al. (2020) detected that these radiograph images' left lower lung area has single nodular opacity.

Zhao et al. (2020) found vascular dilation in the radiograph images. Li and Xia (2020) also reported interlobular septal thickening along with GGO in COVID-19 patients. Analysing the CT images or X-rays for confirmation of COVID-19 can be done by the radiologist. But as the number of images is increasing rapidly, it is very difficult for the radiologists to do the analysis and give a correct and efficient result. To overcome this difficulty the state-of-the-art technology, i.e., deep learning can be used for this process.

2 Related work

Due to the tremendous growth in technology, data is generated at an exponential rate. The processing of such data for applications is error-prone and also have variations among different experts. The solution for this is the application of machine learning techniques for data analysis and extracting features. Brody (2013) has stated that in medical image analysis, computed tomography (CT), X-ray, ultrasound, magnetic resonance (MR), etc., are used for image acquisition and image interpretation is performed by physicians and radiologists. These days radiological images are obtained by higher resolution but the interpretation of such images manually is error-prone. To overcome this, a subset of machine learning, deep learning is widely used in medical imaging. Deep learning is an effective supervised machine learning approach. Schmidhuber (2015) has given an overview of a variety of neural networks, i.e., deep neural network model. The basic computational unit of this approach is a neuron. Neuron accepts multiple inputs as signals and combines these inputs linearly using weights. The combined signal is passed through nonlinear operations and finally, the output is generated. This is regarding a single neuron in a layer. But in deep learning, more layers are present each with multiple neurons. Shen et al. (2017) have reviewed deep learning methods used in medical images, which helps in identifying, classifying and finding patterns in medical images. LeCun et al. (2015) stated that deep learning is popular because of its architecture which helps to learn features and classify images from the input data in one pipeline. Chauhan et al. (2018) used the convolutional neural network (CNN), which is a popular example of a deep neural network in image recognition and image classification application. Detection of important features automatically without human intervention is the main advantage of CNN. Krizhevsky et al. (2012) have introduced a pre-trained deep CNN model, which can be used in image classification and recognition.

The following literature has shown the use of deep learning in detecting COVID-19 patients by using X-ray images. Ghoshal and Tucker (2020) obtained 70 lung X-ray images of COVID-19 positive patients and pneumonia, i.e., non-COVID-19 X-ray. Cohen et al. (2020) made this COVID-19 positive patients X-ray collection. By using Bayesian inference with the basic VGG16 model, the authors have proposed a Bayesian CNN model for detecting COVID-19. This improved the accuracy from 85.7% to 92.9%. To help comprehend the working of deep learning model, the authors have generated saliency maps to show the locations which are getting focused on deep learning. Narin et al. (2020) proposed the use of three CNN models: ResNet50, InceptionResNetV2 and InceptionV3 to screen COVID-19 positive patients. The authors have taken two classes, i.e., COVID-19 X-ray images and pneumonia X-ray images. Fifty images from each category were taken in this work. They showed that ResNet50 attains the best classification accuracy with 98.0% followed by 97.0% by InceptionV3 and 87.0% by InceptionResNetV2. Zhang et al. (2020) proposed a model based on ResNet. This work has also considered X-ray images of COVID-19 positive and non-COVID-19 (pneumonia) patients. The authors have achieved an area under curve (AUC) of 0.952, sensitivity of 96.0% and specificity of 70.7%. Wang and Wong (2020) proposed a deep CNN model and named it COVID-Net that achieves an accuracy of 83.5% on X-ray images to detect COVID-19. The dataset used includes four categories: healthy people, bacterial pneumonia patients, viral pneumonia patients and COVID-19 patients. Jin et al. (2020) uses CT scan images of COVID-19 positive patients and COVID-19 negative persons. The authors used a 2D CNN-based model for segmentation of lung slices that are then classified. They have shown a specificity of 95.5%, sensitivity of 94.1% and AUC of 0.979. Hemdan et al. (2020) proposed a COVIDX-Net model to detect COVID-19 positive patients in the X-ray images. They have employed a deep learning model and used seven CNN models in the proposed method. Sethy and Behera (2020) extracted features by using different CNN models and classified them using the classifier support vector machine (SVM). They have used X-ray images and shown that the combination of the ResNet50 model's features and SVM classification yields the best result.

3 Our approach

We have considered chest X-ray images from two categories *COVID-19* positive patients and *normal* persons. The X-ray images are processed and classified with the use of transfer learning on pre-trained CNNs. The pre-trained CNNs are trained on the ImageNet dataset. The purpose of using pre-trained CNNs is the unavailability of an adequate number of X-ray images of COVID-19 positive patients required to train a CNN from scratch. Kümmerer et al. (2014) have stated that to make the pre-trained net suitable for a specific purpose, transfer learning should be applied. Because of a limited number of images, k-fold cross-validation is used as well, where k is taken to be 5. For evaluation, we have taken four pre-trained CNNs, XceptionNet, InceptionResNetV2, InceptionV3 and ResNet50. The entire process is given in Algorithm 1. We have proposed four modifications to the ResNet50 model mentioned below. The proposed method is also given as a block diagram in Figure 1.

Figure 1 Block diagram of the proposed method (see online version for colours)

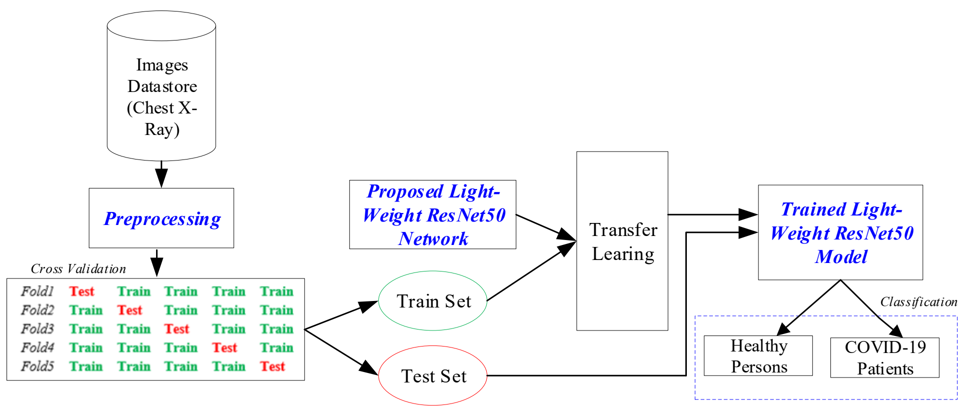

Method-1 (LightWeightResNet50-1)

The last residual block of ResNet50 pre-trained network is removed, i.e., the 16th block, which has three convolutional layers, each followed by a block normalisation layer and reLu layer. The motivation towards the removal of this block is that it reduces overfitting of the model. The existing ResNet50 model structure has more complexity than required for our purpose. Thus removal of a residual block aided in improved performance both in terms of accuracy as well as computation time.

Method-2 (LightWeightResNet50-2)

The 3 × 3 maxpool layer is removed from ResNet50. Maxpool is applied to downsample the feature map produced by the preceding layer. In this process, some features are lost. The intention of removing this layer is to get the complete feature map.

Mehtod-3 (LightWeightResNet50-3)

It is the combination of method-1 and method-2. The last residual block as well as the 3 × 3 maxpool layer is removed from ResNet50. This gives reduced overfitting and detailed feature representation.

Algorithm 1:

Step-1: (Pre-processing) Resize the images in the dataset to that of CNN's input layer size.

Step-2: Randomly divide the data into five groups, i.e., D1, D2, …, D5.

Step-3: Apply five-fold cross-validation: -

i. For each unique group D_i

ii. Test set – D_i and training set – group D_j $1 \le j \le 5$ and $i \ne j$ into one set.

iii. Apply transfer learning on the pre-trained CNN model (existing or modified).

iv. Get the predicted label and prediction score for the test set D_i, i.e., COVID-19/Normal.

v. Compare the actual and predicted labels to generate a confusion matrix.

vi. Obtain true positive, false negative, false positive and true negative from the confusion matrix and calculate $Accuracy_i$, $Recall_i$, $Specificity_i$, $Precision_i$ and $F1\text{-}score_i$ by using equation (1) to (5).

vii. end

Step-4: Calculate the mean accuracy, mean recall, mean specificity, mean precision and mean F1-score of the method by taking individual value from all five-folds.

Method-4 (LightWeightResNet50-4)

The first convolution layer of ResNet50 has a receptive field of 7 × 7. This layer is replaced by three convolution layers each with a 3 × 3 receptive field. This modification is done because if the initial convolution layer's receptive field is large; it skips a lot of information. In CNN, as we go deeper, features are built on the feature maps produced by preceding layers. A smaller receptive field such as 3 × 3 in the initial convolution layer retains more information. Therefore, this is utilised by the deeper layers to produce a detailed feature map.

$$Accuracy = \frac{(TP + TN)}{(TP + FN + FP + TN)} \tag{1}$$

$$Recall = \frac{TP}{(TP + FN)} \tag{2}$$

$$Specificity = \frac{TN}{(TN + FP)} \tag{3}$$

$$Precision = \frac{TP}{(TP + FP)} \tag{4}$$

$$F1\text{-}score = 2 * \frac{(Precision * Recall)}{(Precision + Recall)} \tag{5}$$

4 Experiments and results

In this work, chest X-ray images of 50 COVID-19 positive patients have been obtained from the open-source GitHub repository shared by Cohen (2020). This repository consists of chest X-ray/CT images of patients with acute respiratory distress syndrome (ARDS), COVID-19, Middle East respiratory syndrome (MERS), pneumonia, severe acute respiratory syndrome (SARS). In addition to this, 50 normal chest X-ray images were selected from the Kaggle Repository (2020) called ‘chest X-ray images (pneumonia)’. Sample images of COVID-19 positive and normal are shown in Figure 2 and Figure 3 respectively.

Figure 2 Sample X-ray images of COVID-19 positive patients

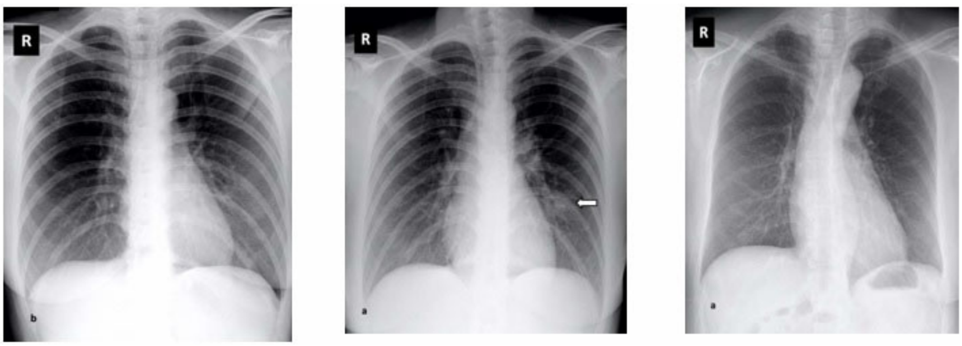

Figure 3 Sample X-ray images of normal persons

4.1 Experimental setup

Training parameters such as batch size is set as 2, the learning rate is 10^{-5} and the number of epochs is set to 30. The optimiser used is *Adam* for training CNNs. As transfer learning is used, training is completed with less number of epochs. The CNNs are trained using NVIDIA Geforce RTX 2070 16 GB GPU on MATLAB R2019a.

4.1.1 Reproducible results in CNN

The neural network models are stochastic by design. This implies that the networks use randomness such as random initialisation of weights. Randomness in the system ensures that a better approximation of the function used in the network can be learned. Therefore, the outcome of a network trained on the same data can be different when executed more than once. This is termed as irreproducible results in CNN. As our method is applied on COVID-19 detection purpose, the results of CNN are required to be consistent when trained on the same data, termed as reproducible results. This is achieved by:

1. seeding the random number generator
2. setting the shuffle field in training options to 'never'.

4.2 Performance metrics

In our work, we have two classes (labels), i.e., COVID-19 and normal. The trained model predicts these two labels for any given test image. Given the actual label and the predicted label, a 2 × 2 matrix called a confusion matrix is generated.

The values of the confusion matrix are:

- *true positive (TP)* – a COVID-19 positive X-ray image is classified as COVID-19
- *false negative (FN)* – a COVID-19 positive X-ray image is classified as normal
- *false positive (FP)* – a normal X-ray image is classified as COVID-19
- *true negative (TN)* – a normal X-ray image is classified as normal.

By using these four values, five parameters are obtained:

- *accuracy:* it is the fraction of images that were correctly predicted by the model
- *recall:* it gives a measure of positive images correctly predicted
- *specificity:* it gives a measure of negative images correctly predicted
- *precision:* it gives a measure of positive predicted images that are positive
- *F1-score:* it gives the harmonic mean of precision and recall.

As the confusion matrix is produced after each test, five individual confusion matrices are obtained for each of the folds. Therefore, TP, FN, FP and TN are taken from confusion matrix values fold-wise. These values are given in Table 1.

Table 1 TP, FN, FP and TN for each fold of the methods

Method	*Fold-1*				*Fold-2*				*Fold-3*				*Fold-4*				*Fold-5*			
	TP	*FN*	*FP*	*TN*	*TP*	*FN*	*FP*	*TN*	*TP*	*FN*	*FP*	*TN*	*TP*	*FN*	*FP*	*TN*	*TP*	*FN*	*FP*	*TN*
XceptionNet	4	6	0	10	7	3	0	10	6	4	0	10	9	1	3	7	7	3	0	10
Inception ResNetV2	4	6	7	3	2	8	0	10	8	2	0	10	3	7	0	10	7	3	0	10
InceptionV3	3	7	1	9	7	3	2	8	8	2	2	8	1	9	1	9	7	3	4	6
ResNet50	9	1	1	9	9	1	1	9	1	9	0	10	7	3	0	10	10	0	0	10
LightWeightResNet50-1	10	0	2	8	10	0	2	8	2	8	0	10	10	0	0	10	10	0	0	10
LightWeightResNet50-2	9	1	0	10	10	0	2	8	10	0	0	10	10	0	0	10	10	0	0	10
LightWeightResNet50-3	10	0	1	9	10	0	1	9	10	0	0	10	10	0	0	10	10	0	0	10
LightWeightResNet50-4	9	1	1	9	10	0	2	8	10	0	1	9	9	1	1	9	9	1	1	9

Figure 4 Fold-wise accuracy for all the methods (see online version for colours)

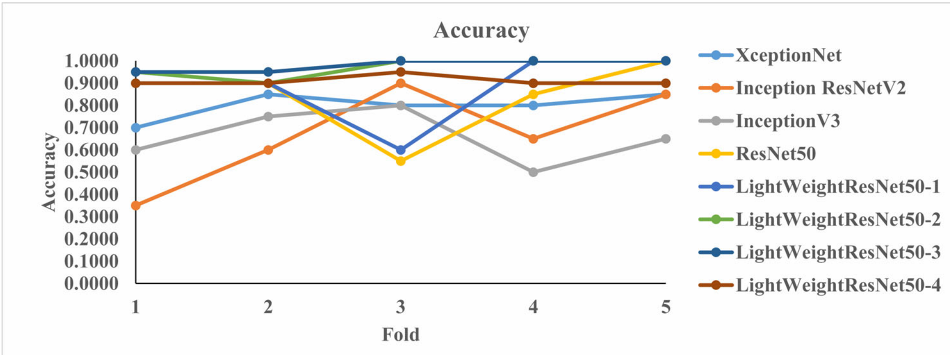

Figure 5 Fold-wise recall for all the methods (see online version for colours)

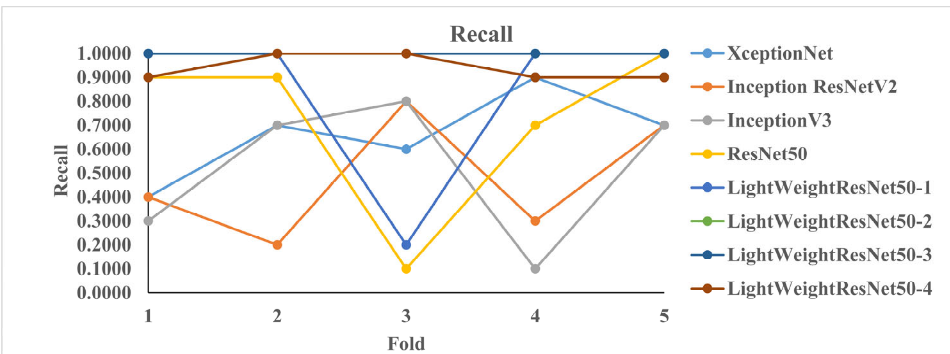

Figure 6 Fold-wise specificity for all the methods (see online version for colours)

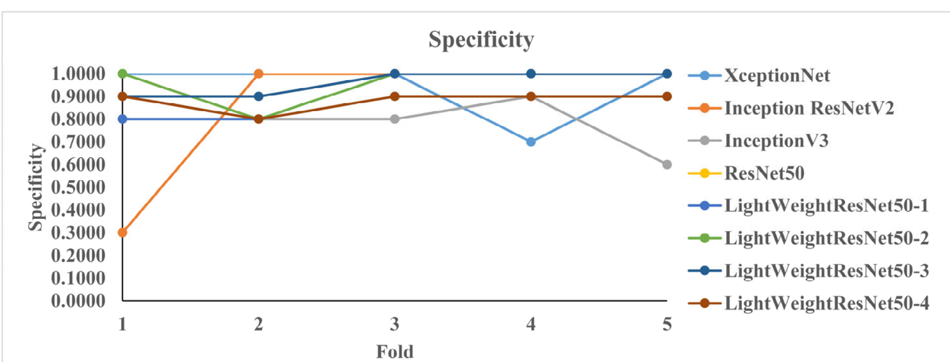

Figure 7 Fold-wise precision for all the methods (see online version for colours)

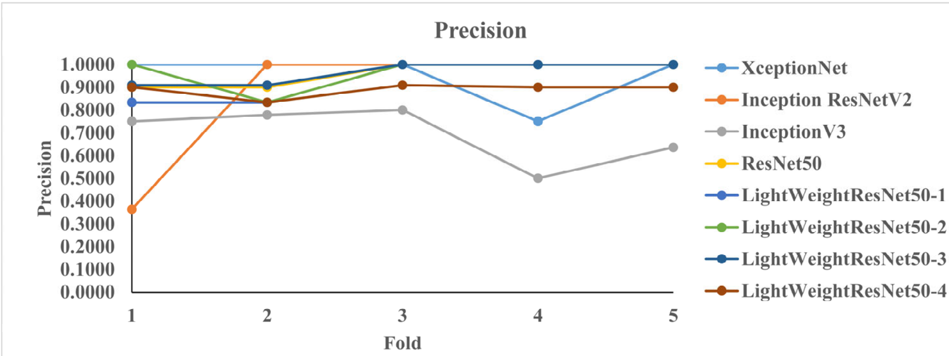

Figure 8 Fold-wise F1-score for all the methods (see online version for colours)

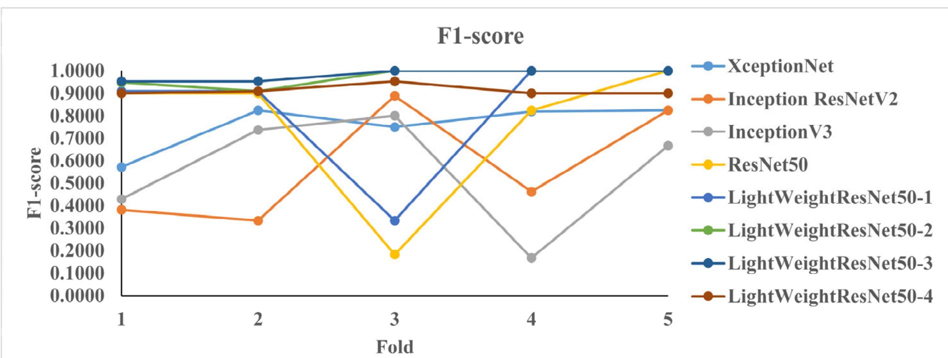

Table 2 Average accuracy, recall, specificity, precision and F1-score for the methods

	Avg. accuracy	*Avg. recall*	*Avg. specificity*	*Avg. precision*	*Avg. F1-score*
XceptionNet	0.8000	0.6600	0.9400	0.9500	0.7573
Inception ResNetV2	0.6700	0.4800	0.8600	0.8727	0.5776
InceptionV3	0.6600	0.5200	0.8000	0.6928	0.5597
ResNet50	0.8400	0.7200	0.9600	0.9600	0.7611
LightWeightResNet50-1	0.8800	0.8400	0.9200	0.9333	0.8303
LightWeightResNet50-2	0.9700	0.9800	0.9600	0.9667	0.9713
LightWeightResNet50-3	0.9800	1.0000	0.9600	0.9636	0.9810
LightWeightResNet50-4	0.9100	0.9400	0.8800	0.8885	0.9123

The five parameters (accuracy, recall, specificity, precision and F1-score) are also obtained for each fold individually for all the methods. The graphs formed by accuracy, recall, specificity, precision and F1-score parameters for five-folds for all the methods are shown in Figure 4, Figure 5, Figure 6, Figure 7 and Figure 8 respectively. Then the average of these parameters is calculated for the methods. The average values are shown in Table 2.

The trained model yields a predicted label as well as a prediction score for each fold. The five labels and scores are used to get a receiver operator characteristics (ROC) curve for each method. Fawcett (2006) introduces *the ROC curve* as: it illustrates graphically the trade-off between TP rate (recall) and false-positive rate (1 – specificity) at each threshold. FPR is plotted on the x-axis whereas TPR is plotted on the y-axis. The point (0, 0) situated at the lower left of the curve represents the classifier delivering zero positive labels. This point implies that the classifier does not contribute to false-positive errors. However, it does not obtain TPs as well. The opposite point, i.e., (1, 1) delivers entirely positive classifications. Perfect classification is represented by the point (0, 1).

Figure 9 ROC curve for all the methods (see online version for colours)

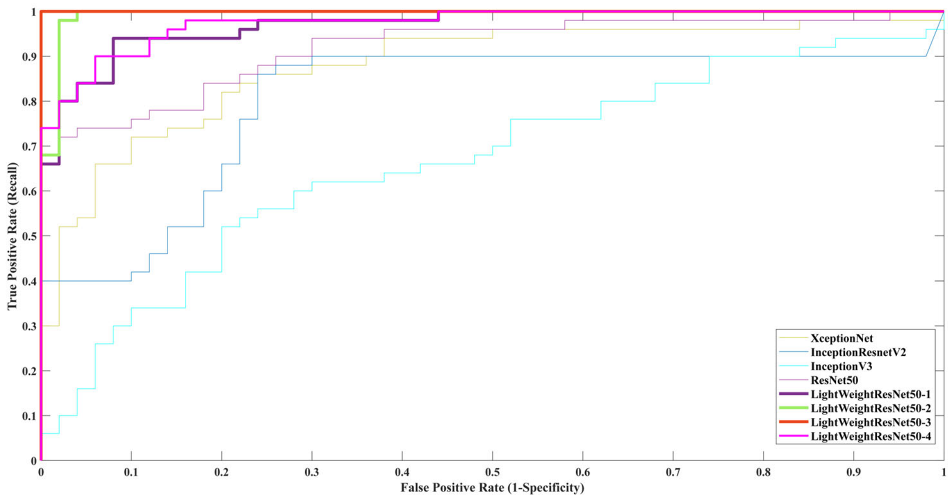

Table 3 AUC values for all the methods

	Area under curve
XceptionNet	0.8788
Inception ResNetV2	0.8022
InceptionV3	0.6672
ResNet50	0.9188
LightWeightResNet50-1	0.9696
LightWeightResNet50-2	0.9932
LightWeightResNet50-3	1.0000
LightWeightResNet50-4	0.9740

AUC: ROC is a probability curve and AUC represents a degree or measure of discriminatory power of the binary class, which shows the classifier's ability to predict the images positive and negative. An AUC of 1 represents a perfect model whereas an AUC of 0.5 portrays a futile model. The model is better at predicting positive as positive and negative as negative indicated by higher AUC. Therefore, the higher the AUC, the better the model is at distinguishing between positive and negative classes. The ROC curve is shown in Figure 9 and the AUC values are given in Table 3.

5 Discussion

In our work, we have shown four existing pre-trained CNN models, i.e., XceptionNet, InceptionResNetV2, InceptionV3, and ResNet50 for comparisons with the proposed methods. InceptionV3 gives the least accuracy of 66%. InceptionResNetV2, XceptionNet and ResNet50 are giving accuracy of 66%, 80% and 84% respectively. The four proposed methods are giving better accuracy than the existing networks considered here. Accuracy yielded by LightWeightResNet50-1, LightWeightResNet50-2, LightWeightResNet50-3 and LightWeightResNet50-4 are 88%, 97%, 98% and 91% respectively. The best accuracy is given by LightWeightResNet50-3 with an improvement of 14% with respect to ResNet50 as shown in Table 2. From the fold-wise TP, FN, FP and TN showed in Table 1, it can be seen that all the four proposed modifications are giving better results. The same can be observed from the fold-wise accuracy, recall, specificity, precision and F1-score graph shown from Figure 4 to Figure 8. It can also be observed from the ROC curve shown in Figure 9 that the curve for the proposed modifications is occupying more AUC. The values of AUC for the individual method is given in Table 3. The proposed LightWeightResNet50-1, LightWeightResNet50-2, LightWeightResNet50-3 and LightWeightResNet50-4 have an AUC of 0.9696, 0.9932, 1.0000 and 0.9740 which is better than the existing CNN models considered in this work.

6 Conclusions and future work

This paper has proposed four different efficient methods for rapid detection of COVID-19 pandemic, where each method is based on a significant modification on ResNet50. In the first method, to overcome the overfitting problem and to reduce the computational cost of the proposed system, the last residual block of ResNet50 is removed. In the second proposed method, maxpool layer of ResNet50 is discarded to gather dense feature information. The third proposed method of this paper is the combination of the first two methods. In the last proposed method, the first 7×7 convolution layer of ResNet50 is replaced with three convolution layers each with a 3×3 receptive field, to find the detailed feature information. The image dataset is created by collection chest X-ray images of 50 coronavirus infected patient and 50 non-infected persons for evaluation of our proposed methods. Each proposed method is compared with three existing methods in terms of ten different performance measures, i.e., TP, FN, FP, TN, accuracy, recall, specificity, precision, F1-score and AUC. All the proposed modifications are giving better performance measures when compared with the existing XceptionNet, InceptionV3, InceptionResNetV2 and ResNet50. The improvements given here are with respect to the best performing existing CNN, i.e., ResNet50. LightWeightResNet50-1 gives 4% accuracy improvement. LightWeightResNet50-2 gives 13% accuracy improvement. LightWeightResNet50-3 gives 14% accuracy improvement. LightWeightResNet50-4 gives accuracy 7% improvement. ROC graph is drawn for all the methods. The proposed four methods are giving an AUC improvement of 5%, 8%, 9% and 6% respectively.

6.1 Future work

As part of future work, the severity assessment of COVID-19 can be done. And also, to improve the time complexity map-reduce paradigm in a distributed environment can be used.

References

Brody, H. (2013) 'Medical imaging', *Nature*, Vol. 502, No. 7473, pp.S81–S81.

Chauhan, R., Ghanshala, K.K. and Joshi, R.C. (2018) 'Convolutional neural network (CNN) for image detection and recognition', in *2018 First International Conference on Secure Cyber Computing and Communication (ICSCCC)*, pp.278–282.

Cohen, J. (2020) *COVID-19 Cases with Chest X-ray or CT Images* [online] https://github.com/ieee8023/covid-chestxray-dataset (accessed 12 May 2020).

Cohen, J.P., Morrison, P. and Dao, L. (2020) *COVID-19 Image Data Collection*, arXiv preprint arXiv: 2003.11597.

Fawcett, T. (2006) 'Introduction to receiver operator curves', *Pattern Recognit. Letters*, Vol. 27, No. 8, pp.861–874.

Ghoshal, B. and Tucker, A. (2020) *Estimating Uncertainty and Interpretability in Deep Learning for Coronavirus (COVID-19) Detection*, arXiv preprint arXiv: 2003.10769.

Hemdan, E.E.D., Shouman, M.A. and Karar, M.E. (2020) *Covidx-Net: a Framework of Deep Learning Classifiers to Diagnose Covid-19 in X-ray Images*, arXiv preprint arXiv: 2003.11055.

Huang, C., Wang, Y., Li, X., Ren, L., Zhao, J., Hu, Y., Zhang, L., Fan, G., Xu, J., Gu, X. and Cheng, Z. (2020) 'Clinical features of patients infected with 2019 novel coronavirus in Wuhan, China', *The Lancet*, Vol. 395, No. 10223, pp.497–506.

Jin, C., Chen, W., Cao, Y., Xu, Z., Zhang, X., Deng, L., Zheng, C., Zhou, J., Shi, H. and Feng, J. (2020) 'Development and evaluation of an AI system for COVID-19 diagnosis', *medRxiv*.

Kaggle Repository (2020) *Chest X-Ray Images* [online] https://www.kaggle.com/paultimothy mooney/chest-xray-pneumonia (accessed 12 May 2020).

Kong, W. and Agarwal, P.P. (2020) 'Chest imaging appearance of COVID-19 infection', *Radiology: Cardiothoracic Imaging*, Vol. 2, No. 1, p.e200028.

Krizhevsky, A., Sutskever, I. and Hinton, G.E. (2012) 'ImageNet classification with deep convolutional neural networks', in *Advances in Neural Information Processing Systems*, pp.1097–1105.

Kümmerer, M., Theis, L. and Bethge, M. (2014) *Deep Gaze I: Boosting Saliency Prediction with Feature Maps Trained on ImageNet*, arXiv preprint arXiv: 1411.1045.

LeCun, Y., Bengio, Y. and Hinton, G. (2015) 'Deep learning', *Nature*, Vol. 521, No. 7553, pp.436–444.

Li, Y. and Xia, L. (2020) 'Coronavirus disease 2019 (COVID-19): role of chest CT in diagnosis and management', *American Journal of Roentgenology*, Vol. 214, No. 6, pp.1280–1286.

Mahase, E. (2020) 'Coronavirus: covid-19 has killed more people than SARS and MERS combined, despite lower case fatality rate', *The BMJ 2020*, Vol. 368, p.m641.

Narin, A., Kaya, C. and Pamuk, Z. (2020) *Automatic Detection of Coronavirus Disease (Covid-19) Using X-ray Images and Deep Convolutional Neural Networks*, arXiv preprint arXiv: 2003.10849.

Nationalgeographic (2020) [online] https://www.nationalgeographic.com/science/2020/02/here-is-what-coronavirus-does-to-the-body/ (accessed 12 May 2020).

Schmidhuber, J. (2015) 'Deep learning in neural networks: an overview', *Neural Networks*, Vol. 61, pp.85–117.

Sciencemag (2020) [online] https://www.sciencemag.org/news/2020/04/nih-launches-competition-speed-covid-19-diagnostics (accessed 12 May 2020).

Sethy, P.K. and Behera, S.K. (2020) *Detection of Coronavirus Disease (Covid-19) based on Deep Features*, Preprints, 2020030300.

Shen, D., Wu, G. and Suk, H.I. (2017) 'Deep learning in medical image analysis', *Annual Review of Biomedical Engineering*, Vol. 19, No. 1, pp.221–248.

Technology Networks (2020) [online] https://www.technologynetworks.com/diagnostics/blog/developing-antibodies-and-antigens-for-covid-19-diagnostics-333088 (accessed 12 May 2020).

Wang, L. and Wong, A. (2020) *COVID-Net: a Tailored Deep Convolutional Neural Network Design for Detection of COVID-19 Cases from Chest Radiography Images*, arXiv preprint arXiv: 2003.09871.

WHO (2020a) *COVID-19* [online] https://www.who.int/emergencies/diseases/novel-coronavirus-2019 (accessed 12 May 2020).

WHO (2020b) *COVID-19 Questions and Answers* [online] https://www.who.int/emergencies/diseases/novel-coronavirus-2019/question-and-answers-hub/q-a-detail/q-a-coronaviruses (accessed 12 May 2020).

Wong, H.Y.F., Lam, H.Y.S., Fong, A.H.T., Leung, S.T., Chin, T.W.Y., Lo, C.S.Y., Lui, M.M.S., Lee, J.C.Y., Chiu, K.W.H., Chung, T. and Lee, E.Y.P. (2020) 'Frequency and distribution of chest radiographic findings in COVID-19 positive patients', *Radiology*, Vol. 296, No. 2, pp.E72–E78.

Worldometers (2020) [online] https://www.worldometers.info/coronavirus (accessed 12 May 2020).

Yoon, S.H., Lee, K.H., Kim, J.Y., Lee, Y.K., Ko, H., Kim, K.H., Park, C.M. and Kim, Y.H. (2020) 'Chest radiographic and CT findings of the 2019 novel coronavirus disease (COVID-19): analysis of nine patients treated in Korea', *Korean Journal of Radiology*, Vol. 21, No. 4, pp.494–500.

Zhang, J., Xie, Y., Li, Y., Shen, C. and Xia, Y. (2020) *Covid-19 Screening on Chest X-ray Images Using Deep Learning Based Anomaly Detection*, arXiv preprint arXiv: 2003.12338.

Zhao, W., Zhong, Z., Xie, X., Yu, Q. and Liu, J. (2020) 'Relation between chest CT findings and clinical conditions of coronavirus disease (COVID-19) pneumonia: a multicenter study', *American Journal of Roentgenology*, Vol. 214, No. 5, pp.1072–1077.

Zu, Z.Y., Jiang, M.D., Xu, P.P., Chen, W., Ni, Q.Q., Lu, G.M. and Zhang, L.J. (2020) 'Coronavirus disease 2019 (COVID-19): a perspective from China', *Radiology*, Vol. 296, No. 2, pp.E15–E25.